Available online at www.sciencedirect.com

ScienceDirect

IFAC Papers Online CONFERENCE PAPER ARCHIVE

IFAC PapersOnLine 53-2 (2020) 12751–12756

Robust local controllers design for the AC grid voltage control of an offshore wind farm ⋆

Carlos Díaz-Sanahuja * **Ignacio Peñarrocha-Alós** * **Ricardo Vidal-Albalate** *

* *Department of System Engineering and Design, Jaume I University, 12071, Castelló de la Plana, Spain (e-mail: csanahuj@uji.es; ipenarro@uji.es; rvidal@uji.es).*

Abstract: In this paper we deal with the problem of voltage control of the AC grid in an offshore wind farm by means of several converters, all of them connected to the AC offshore grid at the Point of Common Coupling (PCC) through different transmission lines. We propose to control the voltage simultaneously by all the connected converters, i.e., we have multiple actuators with the same goal. However, the number of operative converters can change during the wind farm operation and dynamics changes. Thus, it is necessary to assure the stability of the whole system in all different scenarios. In order to achieve a global design and implementation strategy, we propose the use of same controller parameters for all converters. For this kind of wind farm topology, we address the design of controllers as an optimization problem where we seek to maximize the robustness against uncertainty in the model of transmission lines and changes in the number of connected wind turbines guaranteeing the stability of the whole system in all different scenarios as well as a given settling time. Due to the proposed design strategy it is not necessary communication between different converters and controllers do not need to be re-tuned when the number of connected converters changes.

Keywords: Voltage and frequency control, power-system control, robust control, electrical networks, renewable energy systems.

1. INTRODUCTION

In recent years there has been a large expansion of offshore wind farms. According to the European Wind Energy Association, in 15 years the power installed in offshore wind farms will exceed the power installed in onshore Wind Power Plants (Association et al. (2012)). Integration of renewable energy sources is producing important changes into the power grid. Major changes comes from the replacement of generation based on synchronous machines by renewable generation interfaced to the grid via power electronics. The use of Voltage Source Converters (VSCs) based on Modular Multilevel Converters (MMCs) is prevailing over other technologies (Gomis-Bellmunt et al. (2011)) thanks to the important advantages in terms of its control and performance capabilities. This greater controllability of VSCs is important to develop better control strategies for the wind farms and meet the new requirements imposed to this type of systems. In this sense, the network code for connection of generators (Network (2012)) published by European Network of Transmission System Operators for Electricity (ENTSO-E), establishes different requirements for the performance of wind generators. Some of these requirements are: frequency control support, voltage control support, black-start capability or islanded operation among others. Therefore, both for black-start and for islanded operation, we will have to be able to control frequency and voltage by means of local controllers of different interconnected VSCs. Then, voltage and frequency control can be formulated as a problem of designing decentralized regulators which stabilize the system despite of the electrical coupling between VSCs. This topic has been vastly studied in the field of the microgrids and the most standard approaches are based in so-called droop control (Guerrero et al. (2013)) which mimics physic characteristics and controls of traditional synchronous machines. These droop controllers has a simple implementation and do not require synchronization signals. However, they have some drawbacks, e.g., they need to generate frequency and voltage amplitude deviations in order to share the active an reactive power demanded by the loads among the different converters. To eliminate these deviations it is required the use of secondary distributed controllers (Guerrero et al. (2013)) to restore system frequency and voltage to their desired values. Another critical issue is the stability. In the context of droop control, this aspect has been investigated in (Simpson-Porco et al. (2013); Schiffer et al. (2014)). Other approaches that are being studied are the non-droop controllers based on the system model (Riverso et al.

⋆ The present work was supported by the Spanish Ministry of Science, Innovation and Universities and EU FEDER Funds under grant DPI2017-84503-R; by IDIFEDER/2018/036 project, action co-financed by the European Union through the European Regional Development Fund (ERDF) Operating Programme of the Valencian Community 2014-2020; by the Spanish MECD (Grant FPU16/03505) and the Universitat Jaume I (Project UJI-B2018-39)

10.1016/j.ifacol.2020.12.1910

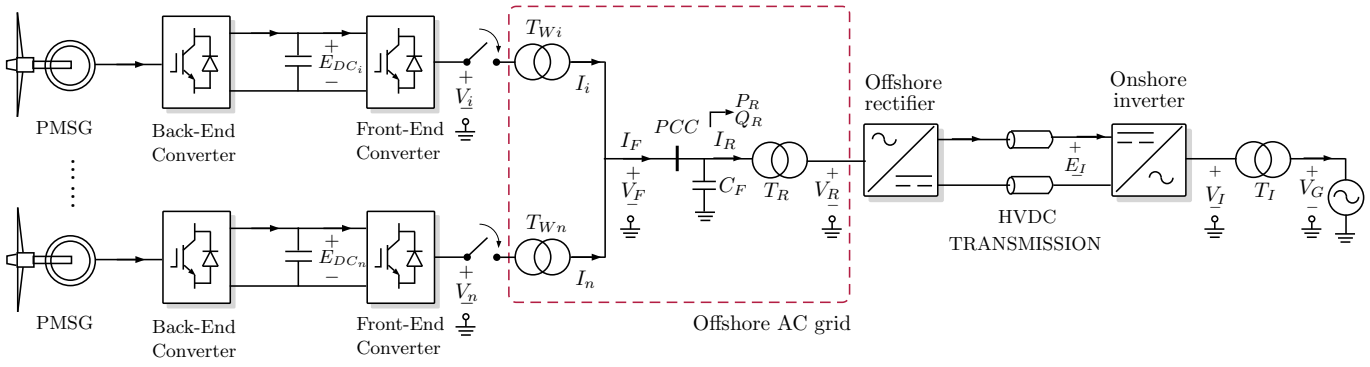

Fig. 1. Offshore wind farm model with a HVDC link.

(2015); Sadabadi et al. (2017)).These controllers require to be synchronized but they enjoy inherent stability and robustness properties. Many of these approaches take into account the behavior when connection and disconnection of loads or sources occurs, or when the topology changes. This kind of approaches have been termed as Plug-and-Play (PnP). In this paper, we propose a strategy that belongs to latter approaches. We aim to control the frequency and voltage of the AC grid of an offshore wind farm with a topology where all converters are connected to the PCC through power lines (see Fig.1). The number of operative converters can change over time, and we have to assure the stability in all possible scenarios. Therefore, to carry out the control, we propose local controllers that neither have to be re-tuned when a connection/disconnection occurs nor communication between controllers is needed. For this purpose it will be necessary to solve an optimization problem posed via matrix inequalities where we will seek the most robust controller that assures stability in all possible scenarios and meets the performance requirements, i.e., a given settling time.

2. PROBLEM STATEMENT

2.1 Offshore wind farm model and control objectives

The model of an offshore wind farm is shown in Fig. 1. The system can be divided into four subsystems. The first subsystem includes the back-end rectifiers of the wind turbines and the DC link of the back-to-back converters. The second one consists of the wind turbine front-end inverters, which generate an AC voltage V_i, and the output transformers T_{Wi} that raise the voltage. The third subsystem is formed by the offshore AC grid which is modeled by means of a capacitor C_F which takes into account the capacitive behavior of the undersea cables, a transformer T_R that raises the voltage and the MMC-VSC rectifier that converts the AC currents into DC ones. Finally, the symmetrical monopolar High Voltage Direct Current (HVDC) link transports the energy, the onshore inverter converts DC voltages into AC and a transformer T_I that raises the voltage.

In this work we are focused on the offshore AC grid.We aim to control ω (being $\omega = 2\pi f$ and f the frequency of the AC grid) and the voltage V_F at PCC (see Fig.1) by means of all operative front-end converters of the wind turbines whose voltage generated in their AC terminals can be directly manipulated. Thus, we can model each VSC as an ideal voltage sources and the control actions are voltages V_i ($i \in \{1, \dots, n\}$) shown in Fig. 1. For this offshore wind farm subsystem we consider that the DC voltatge E_{DCi} is controlled by the back-end converters and we assume that requested active and reactive powers (P_R and Q_R respectively) are imposed by the Offshore rectifier using a reference from the Transmission System Operator (TSO) or by a load if we are operating in islanded mode, so we consider them, as well as I_R, as a disturbances.

2.2 Offshore AC grid model

In this Section, we present the electrical model of the offshore AC grid used. We assume three-phase electrical signals without zero-sequence components and balanced network parameters. The single-phase equivalent scheme of the grid is shown in Fig.2. The number of connected wind turbines N can change during the operation from 1 connected wind turbine to the maximum value of connected wind turbines n. Thus, we can define $\mathcal{S} = \{1, ..., N\}$ as the set of indexes of the connected front-end inverters. The offshore AC grid behavior can be modeled by the differential equations ($\forall i \in \mathcal{S}$)

$$\dot{I}_i = \frac{-R_i}{L_i} I_i + \frac{1}{L_i}(V_i - V_F), \tag{1}$$

$$\dot{V}_F = \frac{1}{C} I_C, \tag{2}$$

$$I_C = I_F - I_R, \qquad I_F = \sum_{i \in \mathcal{S}} I_i, \tag{3}$$

where each equation must be understood as a set of three equal equations in which they represent the three phases of the system with the value of the corresponding variable in the corresponding phase. Since we handle three-phase

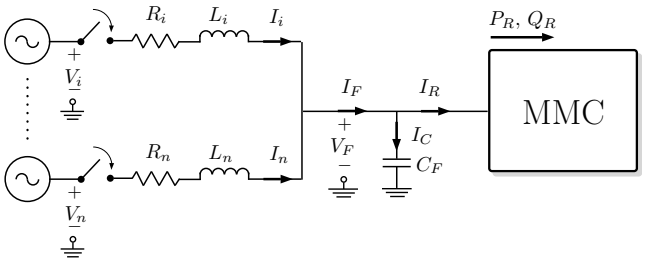

Fig. 2. Single-phase equivalent electrical scheme of the AC offshore grid.

balanced signals, it is interesting to transform the previous model of three equations with sinusoidal variables (i.e., time-varying variables with one equation per phase) into their dq representation (see, e.g., Schiffer et al. (2016)), by means of the well-known Clarke-Park transformation. Hence, the offshore AC grid model defined by (1)-(3) in dq reference frame is ($\forall i \in \mathcal{S}$)

$$\dot{I}_{id} = \frac{-R_i}{L_i} I_{id} + \omega I_{iq} + \frac{1}{L_i} V_{id} - \frac{1}{L_i} V_{Fd}, \tag{4}$$

$$\dot{I}_{iq} = -\omega I_{id} - \frac{R_i}{L_i} I_{iq} + \frac{1}{L_i} V_{iq} - \frac{1}{L_i} V_{Fq}, \tag{5}$$

$$\dot{V}_{Fd} = \omega V_{Fq} - \frac{1}{C_F} I_{Rd} + \frac{1}{C_F} I_{Fd}, \tag{6}$$

$$\dot{V}_{Fq} = -\omega V_{Fd} - \frac{1}{C_F} I_{Rq} + \frac{1}{C_F} I_{Fq}, \tag{7}$$

$$I_{Cd} = I_{Fd} - I_{Rd}, \qquad I_{Fd} = \sum_{i \in \mathcal{S}} I_{id}, \tag{8}$$

$$I_{Cq} = I_{Fq} - I_{Rq}, \qquad I_{Fq} = \sum_{i \in \mathcal{S}} I_{iq}, \tag{9}$$

where subscripts d and q represent the direct and quadrature components of each three-phase signal in (1)-(3). Then, we can compute the active power P_i and reactive power Q_i poured into the network as ($\forall i \in \mathcal{S}$)

$$\begin{bmatrix} P_i \\ Q_i \end{bmatrix} = \begin{bmatrix} V_{Fd} & V_{Fq} \\ V_{Fq} & -V_{Fd} \end{bmatrix} \begin{bmatrix} I_{id} \\ I_{iq} \end{bmatrix}. \tag{10}$$

Hereinafter we will refer to both components of the electrical signals as x_{dq}, representing the vector $x_{dq} = [x_d \ x_q]^T$.

3. PROPOSED APPROACH

3.1 Frequency control

As the offshore AC grid only connects power electronics devices and there are not synchronous machines involved, we propose to keep the frequency fixed at $\omega = \omega^* = 2\pi f^*$ (where f^* is the nominal system frequency) by using a constant switching frequency of the power electronic devices of the converters. Each converter will generate its own angle $\theta(t)$ by means of numerical integration of ω, i.e., $\theta(t) = \int_0^t \omega \, d\tau$. Hence, $\theta(t)$ is used for Clark-Park transformations, so each controller generates its own d and q components for each used variable. The angles generated and used by each controller have to be synchronized by a global synchronization signal that is communicated to the converters through the GPS (Etemadi et al. (2012)). Thus, the frequency ω is considered as a constant and the model (4)-(9) becomes a linear time invariant (LTI) one. In addition, since it is a linear system, the design of the controllers is simpler and its implementation is not so dependent on the noise of the necessary measurable signals or the parametric errors for the linearization, as in (Zhong and Hornik (2012)) where ω is considered as a variable.

3.2 Offshore AC grid voltage control

For the voltage control of the offshore AC grid we propose a control scheme as shown in Fig. 3, where the control of the voltage V_{Fdq} is done by all the front-end inverters. As it can be seen, each voltage controller C_i receives the same

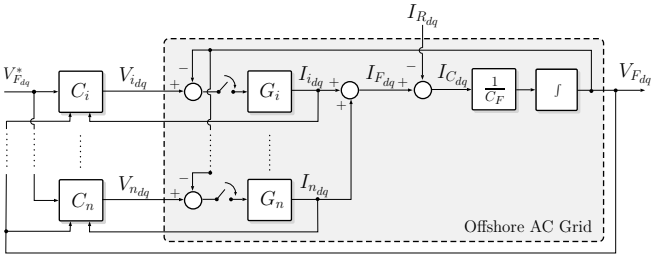

Fig. 3. Offshore AC grid voltage control scheme.

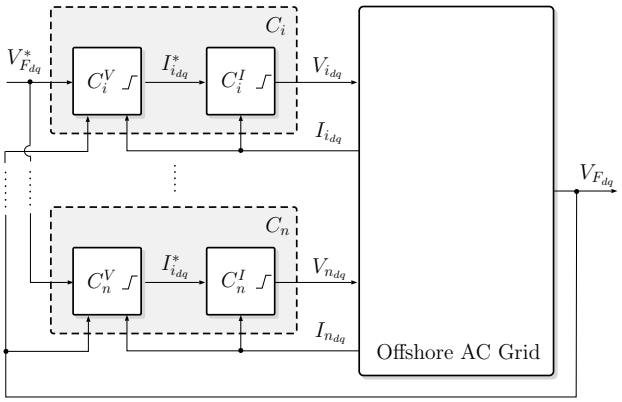

Fig. 4. Cascade control scheme in each front-end inverter.

voltage references V^*_{Fdq} and measurements V_{Fdq}, so, each controller decide the voltages V_{idq} to apply in its terminals with the same goal (i.e., multiple local controllers). In this paper, we have taken some considerations for design purposes. First, we consider that every wind turbine has the same nominal power and that all transmission lines can be modeled with the same parameters R_i and L_i (R and L from now on) so $G_i = G$, $\forall i \in \{1, ..., n\}$, being G_i the transfer function representations of (4) and (5) considering V_{idq} as inputs and I_{idq} as outputs. Additionally, we propose the same control algorithm in each controller of each wind turbine, so $C_i = C$, $\forall i \in \{1, ..., n\}$. We will use these considerations for simplicity on achieving a global design and implementation strategy of the voltage controller and will face it by assuring a given robustness against the imposed modeling error on each line due to the use of common values for R and L. Moreover, in order to protect the front-end inverters, it is necessary to limit currents I_{idq}. We propose a cascade control scheme in each converter with an outer voltage controller C_i^V and an inner current controller C_i^I as shown in Fig. 4. The outputs of the outer voltage controller are the current references I^*_{idq} for the inner current controller, so we can limit them to their nominal values.

Inner current controller. For the inner current controller that generates the voltage V_{idq} for each converter we assume that only the local measurements of I_{idq} are available and that the voltage V_{Fdq} is a non measurable disturbance. We propose a controller with integral term of the form ($\forall i \in \{1, ..., n\}$)

$$V_{idq} = K_x^I I_{idq} + K_q^I \underbrace{\int (I^*_{idq} - I_{idq}) \, dt}_{q_{I_{idq}}}.$$

With the use of model (4)-(5) we can construct an extended model with the integral terms and design with it matrix controllers $K_x^I, K_q^I \in \mathbb{R}^{2\times 2}$. This can be done by standard techniques as Pole Placement or Linear Quadratic Regulator (LQR) assuring certain time response and robustness. We omit the details of this design for brevity.

Outer voltage controller. For the outer voltage controller that generates the current references I_{idq}^* for each front-end inverter we assume that both the local measurements of I_{idq} and $q_{I_{idq}}$, as well as the offshore AC grid voltage measurements V_{Fdq} are available. We propose thus a controller with integral term $q_{V_{Fdq}} = \int (V_{Fdq}^* - V_{Fdq})\, dt$ of the form ($\forall i \in \{1, ..., n\}$)

$$I_{idq}^* = K_I^V \begin{bmatrix} I_{idq} \\ q_{idq} \end{bmatrix} + K_V^V \begin{bmatrix} V_{Fdq} \\ q_{V_{Fdq}} \end{bmatrix}, \tag{11}$$

where $K_I^V \in \mathbb{R}^{2\times 4}$ and $K_V^V \in \mathbb{R}^{2\times 4}$. Note that the term $K_V^V \begin{bmatrix} V_{Fdq} \\ q_{V_{Fdq}} \end{bmatrix}$ although computed locally, will lead to the same value for all the controllers.

For the design of the voltage controller we must model the whole AC grid behavior including all the controllers in the plant, i.e.,

$$\begin{bmatrix} \dot{I}_{idq} \\ \dot{q}_{I_{idq}} \end{bmatrix} = \bar{A}_{II} \begin{bmatrix} I_{idq} \\ q_{I_{idq}} \end{bmatrix} - \frac{1}{L} V_{Fdq} + B_{I^*}\, I_{idq}^* \tag{12}$$

$$\dot{V}_{Fdq} = \frac{1}{C_F}\, I_{Fdq} + \omega J\, V_{Fdq} - \frac{1}{C_F}\, I_{Rdq} \tag{13}$$

with

$$\bar{A}_{II} = \begin{bmatrix} A_{II} & \frac{1}{L} K_q^I \\ -\mathcal{I} & \mathbf{0} \end{bmatrix}, \qquad A_{II} = -\frac{R}{L}\mathcal{I} + \omega J + \frac{1}{L} K_x^I,$$

$$B_{I^*} = \begin{bmatrix} \mathbf{0} \\ \mathcal{I} \end{bmatrix}, \qquad J = \begin{bmatrix} 0 & 1 \\ -1 & 0 \end{bmatrix},$$

where $\mathcal{I}$ and $\mathbf{0}$ are the identity and null matrices of the appropriate size respectively, and where I_{Fdq} results from the addition of the currents of the connected transmission lines, i.e., $I_{Fdq} = \sum_{i\in\mathcal{S}} I_{idq}$. The system dynamics depends on the number of connected transmission lines, that can change during the operation of the wind farm. In this work we will assume that the elapsed time between connections and disconnections is larger than the settling time of the controlled wind farm, so, we only have to assure the system stability for each of the possible number of connected subsystems. Due to the use of the same controller gains (K_x^V and K_q^V) and local controllers, the currents and the integral of tracking errors of the current controllers are not controllable modes from the point of view of the whole wind farm. A controllable subspace for this system is composed of the sum of currents and their tracking error integrals, i.e., of states $I_{Fdq} = \sum_{i\in\mathcal{S}} I_{idq}$ and $q_{I_{Fdq}} = \sum_{i\in\mathcal{S}} q_{I_{idq}}$ plus the AC voltage in the plant. We omit the demonstration for brevity. This controllable subspace can be modeled as

$$\dot{z}_F = \bar{A}_{II}\, z_F - \frac{N}{L} V_{Fdq} + \begin{bmatrix} \mathbf{0} \\ \mathcal{I} \end{bmatrix} I_{Fdq}^* \tag{14}$$

$$\dot{V}_{Fdq} = \frac{1}{C_F} I_{Fdq} + \omega J\, V_{Fdq} - \frac{1}{C_F} I_{Rdq} \tag{15}$$

where $z_F = \begin{bmatrix} I_{Fdq} & q_{I_{Fdq}} \end{bmatrix}^T$ and I_{Fdq}^* is the common control action (addition of local control actions) for this controllable subspace and is given by

$$I_{Fdq}^* = K_I^V\, z_F + N\, K_V^V\, z_V, \;\; z_V = \begin{bmatrix} V_{Fdq} \\ q_{V_{Fdq}} \end{bmatrix}. \tag{16}$$

The closed loop dynamics of this system is given by

$$\dot{\xi} = \mathcal{A}(N)\, \xi + B_r\, r + B_d\, d \tag{17}$$

where the signals are the states $\xi = \begin{bmatrix} z_F & z_V \end{bmatrix}^T$, voltage references $r = V_{Fdq}^*$ and disturbances $d = I_{Rdq}$. As regards the matrices has the following form:

$$\mathcal{A}(N) = \left[\begin{array}{c|cc} \bar{A}_{II} & -\frac{N}{L}\mathcal{I} & \mathbf{0} \\ \hline A_{FI} & \omega J & \mathbf{0} \\ \mathbf{0} & -\mathcal{I} & \mathbf{0} \end{array}\right] + \left[\begin{array}{c} B_{I^*} \\ \hline \mathbf{0} \\ \mathbf{0} \end{array}\right] \begin{bmatrix} K_I^V & K_V^V \end{bmatrix} \begin{bmatrix} \mathcal{I} & \mathbf{0} \\ \mathbf{0} & N\mathcal{I} \end{bmatrix},$$

$$A_{FI} = \frac{1}{C_F} \begin{bmatrix} \mathcal{I} & \mathbf{0} \end{bmatrix}, \; B_r = \begin{bmatrix} \mathbf{0} & \mathbf{0} & \mathcal{I} \end{bmatrix}^T, \; B_d = -\frac{1}{C_F} \begin{bmatrix} \mathbf{0} & \mathcal{I} & \mathbf{0} \end{bmatrix}^T.$$

3.3 Outer voltage controller design.

We address the controller design as an optimization problem in which the objective is to maximize the robustness, not only against variations in the parameters R and L, but also against the number of connected wind turbines N. The idea of maximize robustness against variations in the transmission line parameters comes from the fact of having assumed common R and L for each transmission line. Additionally, we propose robust controllers against the number of operative wind turbines N because, in this way, each controller does not need to know how many wind turbines are connected and it is no necessary to re-tune the controllers when N changes. Also, no communication to know that information is needed. In addition to maximize the robustness, we must fulfill some performance requirements that, in this work, we specify as achieving a given settling time. As a robustness measure against R and L uncertainty we have used the sensitivity margin M_S that is defined as the $\mathcal{H}_\infty$ norm that uses the reference signal $r = V_{Fdq}^*$ as input and the error signal $e = (V_{Fdq}^* - V_{Fdq})$ as output

$$M_S = \sup_r \frac{\|e\|_2}{\|r\|_2}.$$

In order to define this norm we must first add the following equations to model (17), that express the tracking error as a function of the states and reference input

$$e = \mathcal{C}\, \xi + \mathcal{D}\, r \tag{18}$$

with $\mathcal{C} = [\mathbf{0}\ \mathbf{0}\ -\mathcal{I}\ \mathbf{0}]$ and $\mathcal{D} = \mathcal{I}$. Thus, as shown in Boyd et al. (1994), we can guarantee the stability of the system formed by (17) and (18) for the different scenarios and a given sensitivity margin $M_S = \gamma$ if, $\forall N \in \{1, \ldots, n\}$, there exist matrices $\begin{bmatrix} K_I^V & K_V^V \end{bmatrix}$and

$$P_N = P_N^T \succeq 0, \tag{19}$$

that satisfy

$$\begin{bmatrix} \mathcal{A}(N)^T P_N + P_N \mathcal{A}(N) + \mathcal{C}^T\mathcal{C} & P_N B_r + \mathcal{C}^T\mathcal{D} \\ B_r^T P_N + \mathcal{D}^T\mathcal{C} & -\gamma^2\mathcal{I} + \mathcal{D}^T\mathcal{D} \end{bmatrix} \preceq 0. \tag{20}$$

To meet a given settling time we use the Pole Placement in LMI Regions technique consisting of locating the poles λ_N of a system in a desired region of the complex plane. As it is known, the settling time is related with the real part of the dominant pole, so we can approximate

$t_{s_{98}} \simeq -\frac{4}{\max(Re\{\lambda_N\})}$, being $t_{s_{98}}$ the settling time at the 98%. Hence, as described in Chilali et al. (1999), we can set λ_N for all the scenarios in a semi-plane so the real part of them is smaller than α if, $\forall N \in \{1,\dots,n\}$, there exist matrices $\begin{bmatrix} K_I^V & K_V^V \end{bmatrix}$ and

$$Q_N = Q_N^T \succeq 0, \tag{21}$$

that satisfy

$$\mathcal{A}(N)^T Q_N + Q_N \mathcal{A}(N) + 2\,\alpha\, Q_N \preceq 0. \tag{22}$$

Then, we can choose $\alpha = -\frac{4}{t_{s_{98}}}$ to meet the required $t_{s_{98}}$.

With this, we can formulate an optimization problem in which we look for the most robust controller that fulfills the stability and performance $\forall N \in \{1,\dots,n\}$

$$\underset{\gamma,\,P_N,Q_N,K_I^V,K_V^V}{\text{minimize}} \quad \gamma \quad \text{s.t} \quad (19),(20),(21),(22) \tag{23}$$

The optimization problem (23) is not convex and cannot be convexifyied due to the use of a common controller gain for different scenarios (it depends on N as seen in $\mathcal{A}(N)$) and for the use of several Lyapunov matrices (P_N and Q_N for (20) and (22), respectively). Thus, it is not possible to solve the optimization problem by using LMI algorithms with ensured solution. Hence, it is necessary to use heuristic algorithms, iterative algorithms over LMIs like Cone Complementary Linearization (CCL) (El Ghaoui et al. (1997)) or P-K iterations. In this work we have implemented CCL algorithm and a line search over γ.

4. SIMULATION RESULTS

In this Section we provide some simulation results illustrating the behavior of the proposed control in different situations like: changes in the voltage references V_{Fdq}^*, changes in P_R and Q_R and connection/disconnection of some wind turbines. To do that, we use the Simulink toolbox Simscape Power Systems. For each simulation we show the V_{Fdq} response, active power P_i and reactive power Q_i poured to the AC grid by each converter and the behavior of the measured frequency f of the AC grid voltage V_F. The values of the electrical and design parameters used are shown in Table 1. In these simulations, we consider that each wind turbine is formed by an aggregation of 8 wind turbines of 5 MVA each one, and we use this value (40 MVA) as the base power. Note that, as it is considered the power of a front-end converter as a base power, the nominal power of the whole wind power plant is 10 p.u.

Table 1. Simulation Parameters

Front-End Inverters		
$R_i = 136.125$ mΩ	$L_i = 5.199$ mH	$S_i = 40$ MVA
Offshore AC grid		
$V_F = 33$ kV	$C_F = 93.535$ μF	$\omega = 100\pi$ rad/s
Performance Requirements		
$t_{s98} = 100$ ms	$n = 10$	

Change of the voltage references. In this simulation, we have considered two scenarios, $N = 2$ and $N = 10$. Fig.5 shows the response of the system when being V_{Fd} and V_{Fq} controlled at 1 p.u and 0 p.u respectively, we change V_{Fd}^* to 0.8 p.u at $t = 0.2$ s and V_{Fq}^* to 0.2 p.u at $t = 0.6$ s. For this simulation we have set $P_R = 1$ p.u. and $Q_R = 0$ p.u. As we can see, the response for $N = 2$ is slower than for $N = 10$ but it still meets the requirement $t_{s98} \leq 100$ ms. there is a high consumption of reactive power by the front-end converters due to the capacitive behavior of the offshore AC grid and the low active power generated.

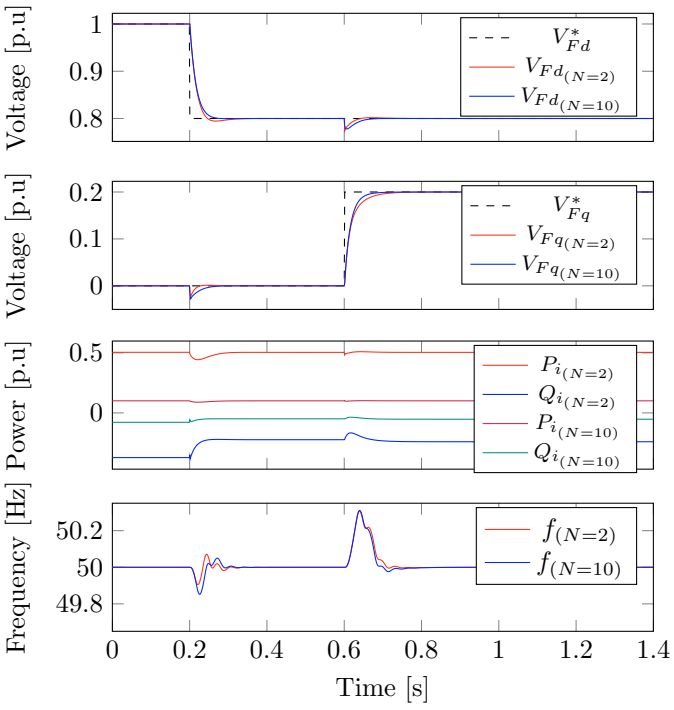

Fig. 5. Change of the voltage references.

Disturbance rejection. To analyze the disturbance rejection of the proposed control, we have applied step changes in the active and reactive power P_R and Q_R. Obviously, during normal operation no such abrupt changes will occur. Fig.6 shows the response of the system when being V_{Fd} and V_{Fq} controlled at 1 p.u and 0 p.u respectively, we change P_R from 1 p.u to 1.5 p.u at $t = 0.2$ s and Q_R from 0 p.u to 0.5 p.u at $t = 0.6$ s. For this simulation, we have considered the same two scenarios (N=2 and N=10). As we can see, the proposed control keeps controlled V_{Fdq}.

Connection/Disconnection of wind turbines. For this simulation, we set $V_{Fd}^* = 1$ p.u, $V_{Fq}^* = 0$ p.u, $P_R = 1.5$ p.u and $Q_R = 0.5$ p.u. Fig.7 shows the response of the system when we connect/disconnect some wind turbines. Simulation begins with $N = 5$ and at $t = 0.2$ s one wind turbine is suddenly disconnected (e.g., due to a sudden trip of a circuit breaker). At $t = 0.5$ s two wind turbines are connected, and at $t = 0.8$ s three of them are disconnected again. As we can see in Fig.7, after each connection/disconnection, there is a redistribution of the power. For sake of clarity, we only show the power of those connected wind turbines.Total active power P_R is dispatched between all connected wind turbines proportionally. There is also a change in reactive power dispatched by each wind turbine, but in these case, we have to consider the effect of the capacitor. We can also see that, despite the change of N, V_{Fdq} remain controlled at their reference values.

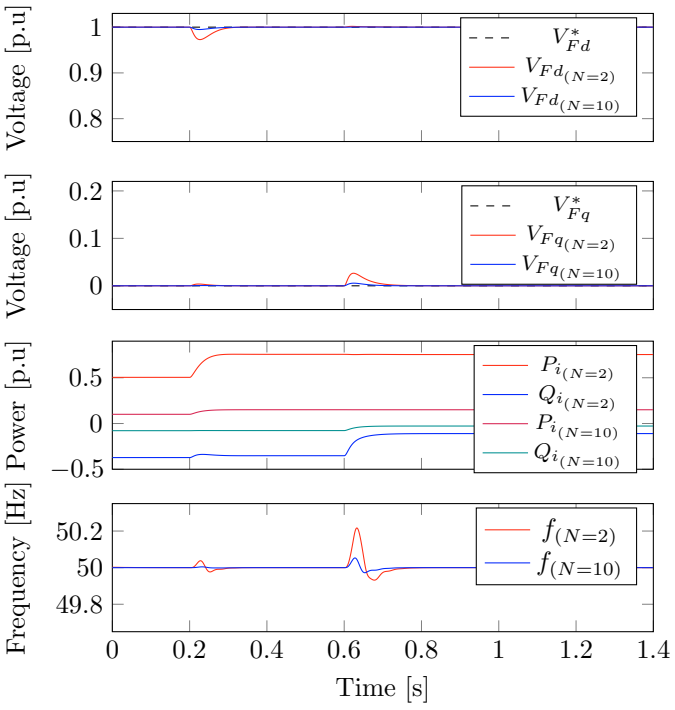

Fig. 6. Disturbance rejection.

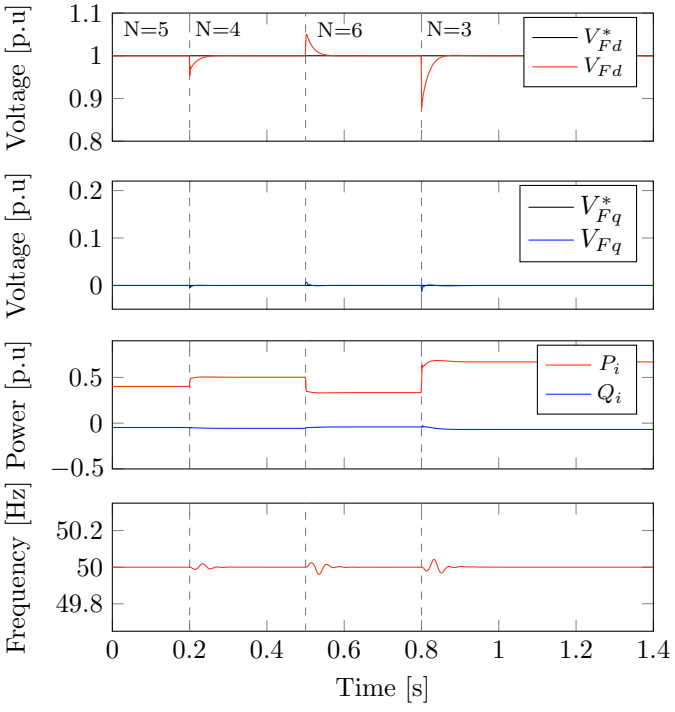

Fig. 7. Connection/Disconnection of wind turbines.

5. CONCLUSIONS

In this paper, we have developed a strategy for designing robust voltage controllers (against uncertainty in the transmission line parameters and the number of operative wind turbines) for the AC grid of an offshore wind farm with a common topology (i.e., all converters connected to the PCC through power lines). This strategy leads us to propose the same controller for all converters and as it is robust against N, it is not necessary communication between controllers and we don't need to re-tune them when N changes. Hence, we can guarantee the stability of the controlled system and fulfill the performance requirements. We have carried out some simulations for different situations and we have proved that with this control strategy, we can track voltage references, we can rejects disturbances and we can change the number of connected wind turbines keeping the system stable.

REFERENCES

Association, E.W.E. et al. (2012). *Wind energy-the facts: a guide to the technology, economics and future of wind power*. Routledge.

Boyd, S., El Ghaoui, L., Feron, E., and Balakrishnan, V. (1994). *Linear matrix inequalities in system and control theory*, volume 15. Siam.

Chilali, M., Gahinet, P., and Apkarian, P. (1999). Robust pole placement in lmi regions. *IEEE Transactions on Automatic Control*, 44(12), 2257–2270.

El Ghaoui, L., Oustry, F., and AitRami, M. (1997). A cone complementarity linearization algorithm for static output-feedback and related problems. *IEEE transactions on automatic control*, 42(8), 1171–1176.

Etemadi, A.H., Davison, E.J., and Iravani, R. (2012). A decentralized robust control strategy for multi-der microgrids—part i: Fundamental concepts. *IEEE Transactions on Power Delivery*, 27(4), 1843–1853.

Gomis-Bellmunt, O., Liang, J., Ekanayake, J., King, R., and Jenkins, N. (2011). Topologies of multiterminal hvdc-vsc transmission for large offshore wind farms. *Electric Power Systems Research*, 81(2), 271–281.

Guerrero, J.M., Chandorkar, M., Lee, T., and Loh, P.C. (2013). Advanced control architectures for intelligent microgrids—part i: Decentralized and hierarchical control. *IEEE Transactions on Industrial Electronics*, 60(4), 1254–1262.

Network, E.E. (2012). Code for requirements for grid connection applicable to all generators. *ENTSO-E: Brussels, Belgium*.

Riverso, S., Sarzo, F., and Ferrari-Trecate, G. (2015). Plug-and-play voltage and frequency control of islanded microgrids with meshed topology. *IEEE Transactions on Smart Grid*, 6(3), 1176–1184.

Sadabadi, M.S., Shafiee, Q., and Karimi, A. (2017). Plug-and-play voltage stabilization in inverter-interfaced microgrids via a robust control strategy. *IEEE Transactions on Control Systems Technology*, 25(3), 781–791.

Schiffer, J., Ortega, R., Astolfi, A., Raisch, J., and Sezi, T. (2014). Conditions for stability of droop-controlled inverter-based microgrids. *Automatica*, 50(10), 2457 – 2469.

Schiffer, J., Zonetti, D., Ortega, R., Stanković, A.M., Sezi, T., and Raisch, J. (2016). A survey on modeling of microgrids—from fundamental physics to phasors and voltage sources. *Automatica*, 74, 135–150.

Simpson-Porco, J.W., Dörfler, F., and Bullo, F. (2013). Synchronization and power sharing for droop-controlled inverters in islanded microgrids. *Automatica*, 49(9), 2603 – 2611.

Zhong, Q.C. and Hornik, T. (2012). *Control of power inverters in renewable energy and smart grid integration*. J. Wiley and Sons-IEEE Press, Chichester.